microparticles. These results demonstrate the utility of these systems in future studies to assess the interplay and time course of multiple growth factors in cartilage repair.

Keywords: Dual growth factor delivery; Degradable hydrogel; Enzymatic degradation; Gelatin microparticles; Cartilage tissue engineering

1. Introduction

Severe cartilage degeneration afflicts an estimated 20.7 million Americans with joint pain and, in some cases, lifelong debilitation [1]. Degeneration may often be initiated by lesions to articular cartilage during sports activities, accidents, or improper joint loading, making this tissue more susceptible to additional injuries [2,3]. This tendency toward repeated injury, coupled with the tissue's low cellularity and isolation from the vascular network's rich supply of bioactive molecules, severely limits intrinsic cartilage repair [4,5]. Accordingly, surgical strategies for repair have focused on accessing the regenerative signaling molecules and cells within the subchondral bone marrow. Unfortunately, these techniques require invasive drilling or abrasion through the overlying articular cartilage and into the marrow, and thus, inflict further tissue damage before any therapeutic effect is achieved. Furthermore, the biomechanical and biochemical properties of the resulting tissue generally fail to match that of uninjured cartilage [3,6].

As an alternative to these harsh surgical techniques, our laboratory has developed a class of novel, injectable materials for the delivery of bioactive molecules to cartilage lesions to enhance tissue repair. These systems are based on oligo(poly(ethylene glycol) fumarate) (OPF), a synthetic polymer which can be used to fabricate biodegradable and biocompatible hydrogels [7,8]. OPF, a water-soluble polymer, can be injected into a defect site and crosslinked in situ at physiological conditions, thereby eliminating the need for invasive implantation and retrieval surgeries. Furthermore, we have shown that gelatin microparticles may be incorporated to these gels at the time of crosslinking to act as enzymatically, digestible porogens to speed scaffold degradation [9]. More specifically, the rate of scaffold degradation may be controlled by altering the crosslinking extent of these microparticles and their loading within the OPF network. Additional research has demonstrated the utility of gelatin microparticles as simultaneous carriers of growth factors within these synthetic hydrogel scaffolds [9,10]. In particular, controlled drug release can be achieved by altering either the microparticle composition or hydrogel mesh size of these delivery systems.

Thus far, these novel release systems have focused on the delivery of transforming growth factor-β1 (TGF-β1), a 25-kDa protein which has been shown to promote the chondrogenic differentiation of progenitor cells [11–13], to increase cartilage extracellular matrix synthesis [14–16], and to enhance chondrocyte proliferation [17,18]. However, numerous other bioactive molecules are involved in the maintenance and repair of articular cartilage. In particular, insulin-like growth factor-1 (IGF-1) has been shown to act primarily in an anabolic fashion to increase proteoglycan and type II collagen synthesis [19–23]. In fact, IGF-1, also know as somatomedin C, was initially discovered as result of its ability to promote sulfate incorporation into proteoglycans [19,21]. Maintenance of the proper level and distribution of proteoglycan networks and collagen fibers in articular cartilage is of utmost importance, since these extracellular matrix components, respectively, impart cartilage tissue with its compressive and tensile strength [2,4,24]. Thus, sustained delivery of IGF-1 provides a potential means to stimulate proteoglycan and collagen synthesis in injured cartilage, enhancing the biomechanical and biochemical properties of repaired tissue.

Accordingly, the following work investigates the delivery of IGF-1 from gelatin microparticles, OPF hydrogels, and OPF–gelatin microparticle composites. In particular, initial studies were performed to identify how gelatin isoelectric point (IEP) and crosslinking extent affect IGF-1 release from microparticles in standard phosphate-buffered saline (PBS) and collagenase-containing PBS (CC-PBS). Upon identification of the appropriate microparticle carrier for IGF-1,

further release studies were performed to assess release from microparticles encapsulated in a network of OPF. To examine IGF-1 diffusion through the OPF network alone, IGF-1 release from OPF hydrogels (with no encapsulated microparticles) was also examined. Additionally, the effect of co-encapsulation of non-loaded microparticles with IGF-1-loaded microparticles in composites was also assessed.

Finally, this technology for the release of IGF-1 was extended towards the development of systems for dual release of TGF-β1 and IGF-1. Since IGF-1 has been shown to function mainly as a progression factor [19–23], effectively stimulating in vitro matrix synthesis when continuously delivered to chrondrocyte cultures for 6 weeks [20], dual release systems were designed to provide sustained delivery of IGF-1 over the course at least 4 weeks. In contrast, since TGF-β1 has been shown to act effectively as a chemotractant [25,26], morphogen [11,12,27], and progression factor [14–16], the carrier of TGF-β1 in these composites was manipulated between the hydrogel or microparticle phase, to achieve varied TGF-β1 release profiles. In addition to assessing how carrier of TGF-β1 affected the release kinetics of this growth factor, further studies were conducted to assess how TGF-β1 release affected IGF-1 release from these systems.

2. Experimental methods

2.1. Gelatin microparticle fabrication

Basic and acidic gelatin (Nitta Gelatin, Osaka, Japan) with respective isoelectric points of 9.0 and 5.0 were used separately to fabricate basic or acidic microparticles according to an established method [28]. Briefly, 5 g gelatin was dissolved in 45 ml distilled, deionized water (ddH_20) by mixing and heating (60 °C). This aqueous gelatin solution was added dropwise to 250 ml olive oil while stirring at 500 rpm. The temperature of the emulsion was then decreased to approximately 15 °C with constant stirring. After 30 min, 100 ml chilled acetone (4 °C) was added to the emulsion. After 1 h, the resulting microspheres were collected by filtration and washed with acetone to remove residual olive oil.

Microspheres were crosslinked in a 0.1 wt.% solution of Tween 80 (Sigma, St. Louis, MO) containing either 10 or 40 mM glutaraldehyde (GA) (Sigma) for 15 h at 15 °C. By altering the GA concentration in this reaction, the crosslinking extent of the resulting microparticles may be systematically controlled [10]. Crosslinked microparticles were collected by filtration, washed with ddH_2O, and then agitated in a 25-mM glycine solution to block residual aldehyde groups of unreacted GA. After 1 h, microparticles were again collected by filtration, washed with ddH_2O, and then vacuum dried overnight. After drying, the microparticles were sieved to obtain particles 50–100 μm in size.

2.2. Microparticle loading

Acidic microparticles crosslinked with 10 mM GA were diffusionally loaded with TGF-β1 following previously established methods [10,28]. In particular, microparticles were partially swollen in aqueous TGF-β1 solutions at pH 7.4. At this pH, the TGF-β1–gelatin binding is enhanced by an ionic complexation between positively charged TGF-β1 (IEP of 9.5) and negatively charged acidic gelatin (IEP of 5.0) [9,29]. However, at physiological pH, a significant charge density is not expected to be associated with IGF-1 (IEP of 7.5). Therefore, both basic and acidic gelatin microparticles were loaded with this growth factor and utilized in release studies to examine their potential as a carrier of IGF-1.

Growth factor loading solutions were composed of trace I^{125} labeled-growth factor (Perkin Elmer Life Sciences, Boston, MA) and unlabeled-growth factor (R&D Systems, Minneapolis, MN) to allow for detection of drug release. Microparticle loading was achieved by adding 5 μl of the growth factor solution per mg dried microparticles. This solution volume is below the microparticles' theoretical, equilibrium swelling volume to allow for complete drug absorption. The resulting mixture was vortexed and incubated at 4 °C for 15 h. A loading solution of 2.38 ng TGF-β1/μl PBS was applied to loaded microparticles with this growth factor. The loading solution for IGF-1-loaded microparticles was composed of 1.19 ng IGF-1/μl PBS. These growth factor concentrations were chosen to provide a total, initial loading of approximately 200 ng TGF-β1/g crosslinked gel and 100 ng IGF-1/g crosslinked gel in composites fabricated for dual growth factor delivery. These

Table 1
Composition and loading of systems for IGF-1 release

Formulation	Gel composition					Total IGF-1 loading (ng IGF-1 per g gel)
	(H) Hydrogel	(10) MPs crosslinked with 10 mM GA		(40) MPs crosslinked with 40 mM GA		
	Loading solution	g MPs per g polymer	Loading solution	g MPs per g polymer	Loading solution	
H_{IGF*}	IGF*	–	–	–	–	100
H_b40_{IGF*}	PBS	–	–	0.20	IGF*	200
$H_b10_b40_{IGF*}$	PBS	0.10	PBS	0.10	IGF*	100

growth concentrations are within the range of those shown to be therapeutic in the treatment of full and partial thickness rabbit and porcine articular cartilage defects [25,30]. For consistency, these respective solutions were applied to all TGF-β1- and IGF-1-loaded microparticles. Accordingly, the total growth factor loading in some formulations varied from the total loading in composites for dual growth factor release. Loadings are shown in Tables 1 and 2. Systems with blank microparticles were loaded with PBS (5 μl PBS/mg dried microparticle).

2.3. *In vitro growth factor release from gelatin microparticles*

IGF-1 release from acidic and basic gelatin microparticles, each crosslinked with 10 mM GA, was assessed in standard PBS or collagenase-containing PBS (CC-PBS). TGF-β1 release from acidic gelatin microparticles was also examined under the same conditions. This enabled comparison of the extent of the IGF-1–gelatin complexation to the TGF-β1–gelatin complexation, which has been shown to persist in standard PBS for at least 4 weeks [10]. The effect of microparticle crosslinking extent on IGF-1 release from microparticles was also assessed.

After the 15-h incubation period, loaded microparticles of the indicated composition were then placed into vials with 3 ml of PBS or 3 ml PBS containing 373 ng bacterial collagenase 1A (E.C. 3.4.24.3, Sigma) per ml. This collagenase concentration was chosen to model tissue collagenase concentrations in the synovial fluid of patients with osteoarthritis [31]. All specimens were agitated on a shaker table (70 rpm) at 37 °C. The supernatant of each specimen was collected and replaced by fresh buffer following a schedule designed to maintain an enzyme activity at least 25% of initial enzymatic activity throughout the study [9].

At each time point, the supernatant of each specimen was analyzed for radioactivity using a gamma counter (Cobra II Autogamma, Packard, Meridian, CT). The amount of growth factor in the supernatant was determined by correlation to a standard curve. Cumulative release was determined by normalizing the total growth factor released at each time point with the sum of the total growth factor released over the course of 28 days and the growth

Table 2
Composition and loading of systems for dual IGF-1 and TGF-β1 release

Formulation	Gel composition					Protein loading	
	(H) Hydrogel	(10) MPs crosslinked with 10 mM GA		(40) MPs crosslinked with 40 mM GA		TGF-β1 (ng TGF-β1 per g gel)	IGF-β1 (ng IGF-β1 per g gel)
	Loading solution	g MPs per g polymer	Loading solution	g MPs per g polymer	Loading solution		
$H_b10_{TGF*}40_{IGF}$	PBS	0.10	TGF*	0.10	IGF	200	100
$H_b10_{TGF}40_{IGF*}$	PBS	0.10	TGF	0.10	IGF*	200	100
$H_{TGF*}10_b40_{IGF}$	TGF*	0.10	PBS	0.10	IGF	200	100
$H_{TGF}10_b40_{IGF*}$	TGF	0.10	PBS	0.10	IGF*	200	100

factor remaining in the specimens at day 28. Release rates were determined by taking the slope of the percent cumulative release curve for each sample over the stated range and averaging the resultant slopes for each formulation. Accordingly, rates are stated in terms of the change in the percent cumulative release per day. For all treatments, n was 4 to 6.

2.4. OPF synthesis and characterization

OPF with an initial number average molecular weight of 21,600±1400 and weight average molecular weight of 144,300±5200 was synthesized according to a method developed in our laboratory [32]. Molecular weight determination was likewise conducted using established procedures for gel permeation chromatography [9] with samples run in triplicate.

2.5. Hydrogel and composite fabrication

The OPF hydrogel and composite formulations assessed during the course of this work are shown in Tables 1 and 2. As indicated, these systems were comprised of at least one of three phases: the OPF hydrogel phase (H), acidic microparticles crosslinked with 10 mM GA (10), and acidic microparticle crosslinked with 40 mM GA (40). Abbreviations of each phase in a given formulation are followed by the subscripts b, TGF, or IGF, and respectively, refer to phases which were blank (loaded with PBS), loaded with TGF-β1, or loaded with IGF-1. Asterisks indicate the use of trace I^{125} labeled-growth factor to detect growth factor release.

All gel formulations were fabricated by first dissolving 0.15 g OPF in 395 μl of PBS containing 14 mg *N,N'* -methylene bisacrylamide (Sigma) as a crosslinking agent. Although crosslinking may proceed solely through the OPF double bonds, methylene bisacrylamide is added to accelerate the reaction. For composite fabrication, 0.2 g gelatin microparticles per g OPF were then added to the polymer solution, and the mixture thoroughly vortexed. For hydrogels with no microparticle component, microparticles were omitted. Finally, for both composites and hydrogels, 118 μl PBS, 51 μl of 0.3 M tetramethylethylenediamine (in PBS) (Sigma), and 51 μl of 0.3 M ammonium persulfate (in PBS) (Sigma) were added to initiate crosslinking. The cytocompatibility of this tetramethylethylenediamine/ammonium persulfate initiating system has previously been demonstrated by the successful encapsulation of rat marrow stromal cells in OPF hydrogels during the time of crosslinking [33,34]. For systems designed with growth factor loading in the OPF hydrogel phase (H), the PBS aliquot in this step contained the appropriate concentration of the desired protein to achieve the loading indicated in Table 1. After vortexing, the suspension was injected into a Teflon mold and incubated at 37 °C. After 10-min incubation, this formulation of OPF forms crosslinked hydrogels or composites [10]. After completion of crosslinking, gels were removed from their mold, and a cork bore used to cut discs of approximately 3 mm in diameter and 1 mm in thickness.

2.6. Single and dual growth factor release from hydrogels and composites in vitro

Initial release studies examined IGF-1 release alone from hydrogels and two composite formulations (Table 1). The first composite formulation, abbreviated H_b40_{IGF*}, was composed of two phases: 0.20 g IGF-1-loaded microparticles (crosslinked with 40 mM GA) per g polymer and the surrounding OPF hydrogel phase. This formulation allowed for examination of the effect of microparticle encapsulation on release kinetics. The second composite formulation, abbreviated $H_b10_b40_{IGF*}$, was composed of three phases: unloaded 10 mM microparticles, IGF-1-loaded 40 mM microparticles, and the surrounding OPF hydrogel phase. For these constructs, the microparticle density was again 0.20 g microparticles per g polymer, with a 1:1 mass ratio between the two microparticle types. IGF-1 release from this composite formulation was examined since dual release systems utilized the same material composition. Accordingly, comparing the release profiles of $H_b10_b40_{IGF*}$ and H_b40_{IGF*} constructs allowed for assessment of the effect of co-encapsulating a population of non-loaded gelatin microparticles on IGF-1 release. Additionally, the IGF-1 release profiles of $H_b10_b40_{IGF*}$ constructs were later compared to IGF-1 release profiles in dual release systems to assess the effect of co-loaded TGF-β1 on IGF-1 release.

As shown in Table 1, dual release systems were based on the three phase composition discussed above, with IGF-1 delivery from encapsulated 40 mM microparticles. TGF-β1 was delivered from either the encapsulated 10 mM microparticles ($H_b10_{TGF}40_{IGF}$) or from the surrounding OPF hydrogel ($H_{TGF}10_b40_{IGF}$). For each dual release formulation, two sets of gels were fabricated to separately follow TGF-β1 and IGF-1 release, as noted with an asterisk in abbreviations. For the first set, the loading procedure was performed with an IGF-1 solution containing trace I^{125} labeled-IGF-1, while loading of the second set was performed with a TGF-β1 solution containing trace I^{125} labeled-TGF-β1. All specimens (for both single and dual release studies) were placed in 3 ml of PBS or CC-PBS and maintained according to the methods described above for release studies with non-encapsulated microparticles. For all formulations, n was 4 to 6.

2.7. Statistical analysis

The F test and Tukey's multiple comparison test ($p<0.05$) was used to statistically compare the cumulative release values and release rates exhibited by the three treatments of non-encapsulated, IGF-1-loaded microparticles [35]. Likewise, these tests were used to compare measured release values and rates in OPF systems for IGF-1 delivery. For dual delivery systems, the F test ($p<0.05$) was used to assess potential statistical differences in IGF-1 release values and rates obtained between the two composite

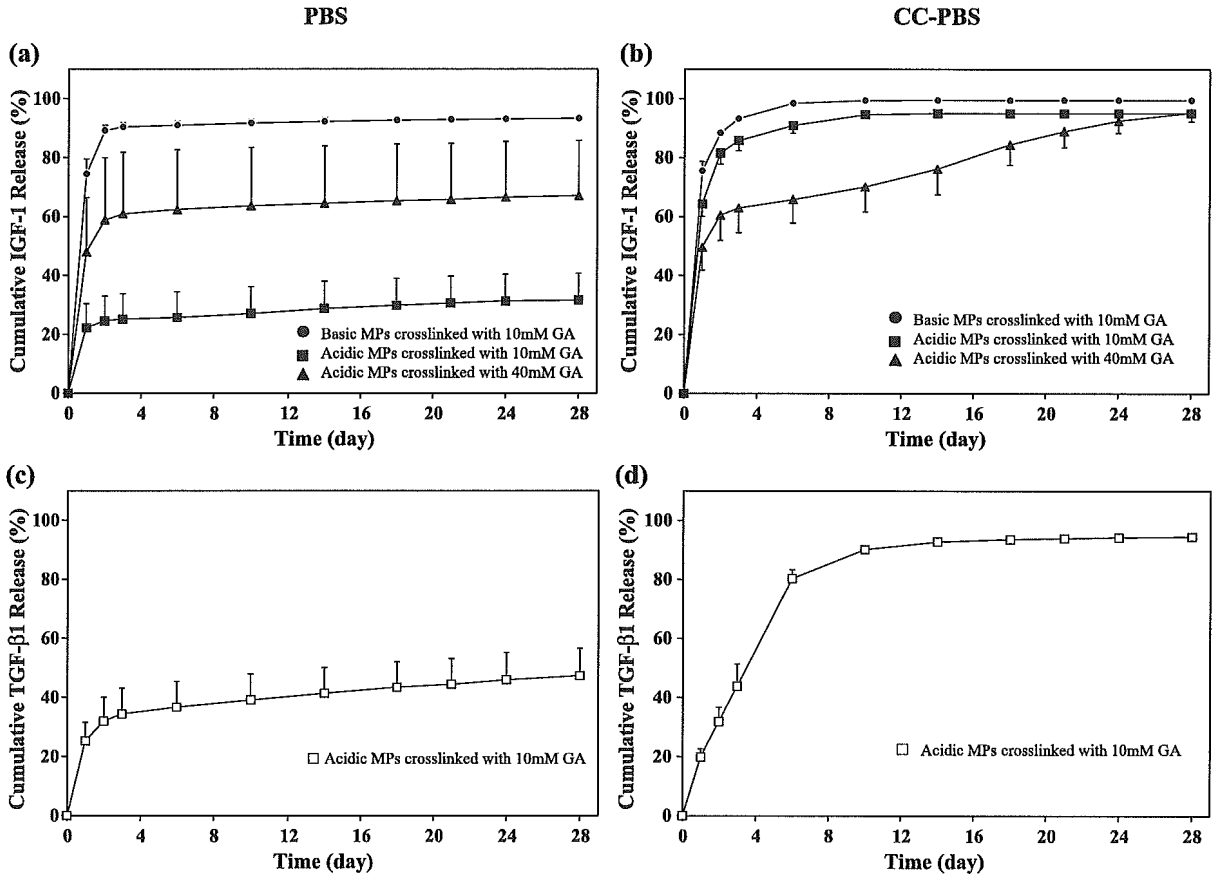

Fig. 1. Effect of gelatin microparticle IEP and crosslinking extent on growth factor release: Average percent cumulative IGF-1 release from microparticles in PBS and in CC-PBS is shown in (a) and (b), respectively, and compared to average percent cumulative TGF-β1 release from microparticles in PBS (c) and in CC-PBS (d). Error bars represent ±standard deviation with n=4 to 6 for each formulation. (a) and (c) PBS. (b) and (d) CC-PBS.

formulations. Potential statistical differences in TGF-β1 release values and rates were assessed in the same manner. For all statistical comparisons, treatments in each buffer were separately compared. Additional statistical analysis was performed as discussed below.

3. Results

To quantify observed trends, release profiles were divided into four phases following the methods of previous investigations [9,10,36]. Phase 1 was clearly defined by a 24 -h burst release from non-encapsulated microparticles, hydrogels, and composites. Distinct release rates were then noted between days 1–3 (Phase 2) and days 6–21 (Phase 3), especially for composites and microparticles in the presence of collagenase. Final cumulative release values were determined to describe the later portion of the observation period (Phase 4) and appeared to correlate well with the extent of visible gel or microparticle degradation.

3.1. In vitro growth factor release from gelatin microparticles

IGF-1 release profiles from basic (IEP=9.0) and acidic (IEP=5.0) gelatin microparticles crosslinked with the indicated GA concentration are shown in Fig. 1a (PBS) and Fig. 1b (CC-PBS). Release studies performed in standard PBS allowed for the evaluation of the extent of the gelatin–IGF-1 complexation. TGF-β1 release from acidic gelatin microparticles (crosslinked with 10 mM GA) was performed as a control since this growth factor is known to have a persistent complexation with acidic gelatin (Fig. 1c). Parallel studies, conducted in CC-PBS, examined the effect of microparticle crosslinking on gelatin digestion and growth factor release.

3.1.1. Release in standard PBS

As shown in Fig. 1a, after only 24 h, basic microparticles crosslinked with 10 mM GA demonstrated a very high burst release (74.4±5.1%). The remaining IGF-1 in these microparticles appeared to diffuse over the next few days, with 90.3±1.4% release by day 3 and 93.3±1.1% by day 28. On the contrary, when acidic gelatin was employed in the fabrication of gelatin microparticles, significantly lower burst release and final cumulative release values were obtained (Table 3a). In fact, the IGF-1 release profile from acidic gelatin microparticles crosslinked with 10 mM GA appeared to correlate well with the observed TGF-β1 release profile (Fig. 1c) from this same microparticle formulation. These results confirmed expectations that gelatin of an IEP below physiological pH would act as a more effective complexation agent due to the slight positive charge character associated with IGF-1 (IEP=7.5) in PBS. It should be noted that microparticle crosslinking extent appeared to affect the extent of complexation as IGF-1 burst release from microparticles crosslinked with 10 mM GA (22.2±8.2%) was statistically lower than burst release from microparticles crosslinked with 40 mM GA (48.0±18.4%). Likewise, final cumulative release in PBS was statistically lower for microparticles crosslinked with 10 mM GA (31.6±9.1%) rather than 40 mM GA (67.1±18.7%).

3.1.2. Release in CC-PBS

However, in the presence of collagenase, the more tightly crosslinked structure of microparticles crosslinked with 40 mM GA appeared to slow enzymatic gelatin digestion and subsequent IGF-1 release when compared to release from less crosslinked 10 mM microparticles. As shown in Fig. 1b and Table 3b, the highest IGF-1 burst (75.5±3.1%) and final cumula-

Table 3
Burst release, phase 2 and 3 release rates, and final cumulative IGF-1 release from various microparticle formulations in PBS (a) and in CC-PBS (b)

Microparticle formulation		Burst release (%)	Phase 2 rate (%/day)	Phase 3 rate (%/day)	Cumulative release (%)
IEP	GA concentration				
(a)					
9	10 mM	74.4±5.1#	8.0±2.0	0.1±0.0^	93.3±1.1#
5	10 mM	22.2±8.2^	1.4±0.3^	0.3±0.1#	31.6±9.1^
5	40 mM	48.0±18.4	6.4±1.3	0.2±0.1	67.1±18.7
(b)					
9	10 mM	75.5±3.1#	8.8±1.3	0.1±0.0	99.5±0.1#
5	10 mM	64.3±4.3	10.7±0.7#	0.2±0.1	95.0±0.6
5	40 mM	49.6±7.8^	6.7±0.5^	1.6±0.2#	95.2±2.9

For each measurement, the highest and lowest values ($p<0.05$) amongst formulations are indicated by (#) and (^), respectively.

tive (99.5±0.1%) release values were observed with basic microparticles, presumably due to their low crosslinking density and poor ability to complex with IGF. Statistically lower burst (64.3±4.3%) and final cumulative (95.0±0.6%) release values were obtained with acidic microparticles crosslinked with 10 mM GA. However, acidic gelatin microparticles crosslinked with 40 mM GA demonstrated the lowest burst release (49.6±7.8%) among all formulations since their tight network structure resists degradation by collagenase.

Trends in Phase 2 and 3 release rates further demonstrated that release and degradation kinetics may be controlled by altering the crosslinking extent of these microparticles. As shown in Table 3b, the Phase 2 release rate (10.7±0.7% per day) for acidic microparticles crosslinked with 10 mM GA was statistically higher than the corresponding rate (6.7±0.5% per day) for microparticles crosslinked with 40 mM GA. However, by the beginning of Phase 3 (day 6), release from the less crosslinked microparticles had risen to approximately 91%, and accordingly, IGF-1 release during this period fell to 0.2±0.1% per day. In contrast, the more crosslinked microparticles exhibited only 66% release by day 6, and thus, demonstrated a Phase 3 release rate of almost ten fold higher (1.6±0.2% per day). Moreover, both TGF-β1 and IGF-1 release (Fig. 1b and d) from acidic microparticles crosslinked with 10 mM GA proceeded with very similar release kinetics in CC-PBS.

3.2. IGF-1 release from hydrogels and composites in vitro

3.2.1. Release in standard PBS

Since acidic microparticles crosslinked with 40 mM GA provided sustained release of IGF-1 for 28 days in CC-PBS, this microparticle formulation was utilized in preparing OPF–gelatin microparticle composites. Fig. 2a provides IGF-1 release profiles from two formulations of composites (H_b40_{IGF*} and $H_b10_b40_{IGF*}$) in standard PBS, as well as the IGF-1 release profile from OPF hydrogels (H_{IGF*}) with no microparticle component. By comparing Figs. 1a and 2a, the dramatic reduction in burst release, obtained by encapsulating these microparticles in a network of OPF, is seen. More specifically, burst release in standard PBS was reduced from approximately 48% with non-encapsulated microparticles to approximately 14% with both formulations of composites. As shown in Table 4a, both composite formulations also exhibited burst release values statistically lower than the burst release from OPF hydrogels (47.0±3.9%). Likewise, the final cumulative release from both composite formulations (44.6±1.4% for H_b40_{IGF*} and 48.3±1.7% for $H_b10_b40_{IGF*}$) was statistically lower than the final cumulative release from OPF hydrogels (79.2±3.3%)

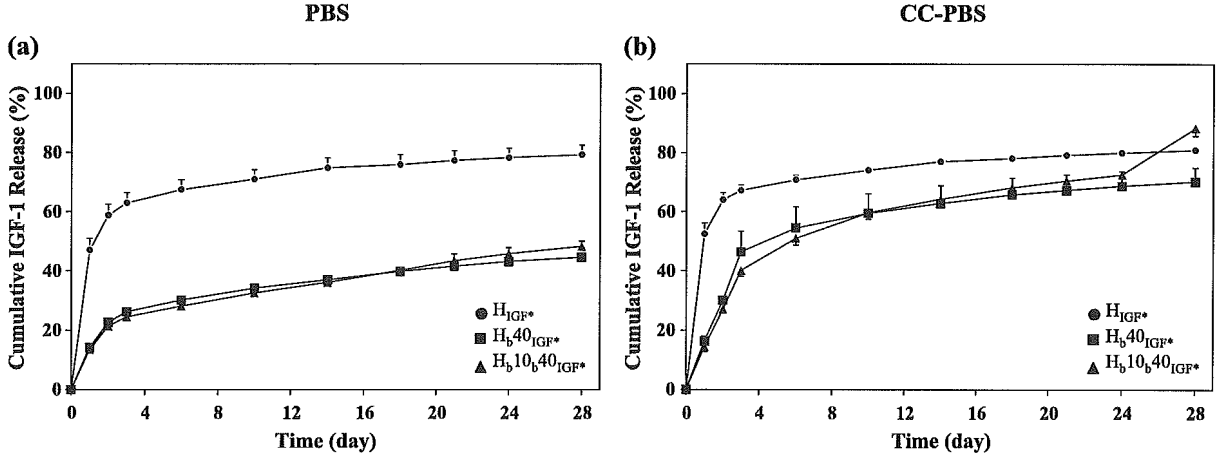

Fig. 2. OPF systems for IGF-1 delivery: Average percent cumulative IGF-1 release from both OPF hydrogels (H_{IGF*}) and two formulations of OPF-gelatin microparticles composites (H_b40_{IGF*} and $H_b10_b40_{IGF*}$) are shown in PBS (a) and in CC-PBS (b). Error bars represent ±standard deviation with n=4 to 6 for each formulation. (a) PBS and (b) CC-PBS.

Table 4
Burst release, phase 2 and 3 release rates, and final cumulative IGF-1 release from OPF hydrogels (H_{IGF*}) and two formulations of OPF–gelatin microparticle composites (H_b40_{IGF*} and $H_b10_b40_{IGF*}$) in PBS (a) and in CC-PBS (b)

Gel formulation	Burst release (%)	Phase 2 rate (%/day)	Phase 3 rate (%/day)	Cumulative release (%)
(a)				
H_{IGF*}	47.0±3.9#	8.0±0.9#	0.6±0.0	79.2±3.3#
H_b40_{IGF*}	14.2±0.4	6.0±0.3	0.8±0.1	44.6±1.4^
$H_b10_b40_{IGF*}$	13.5±0.4	5.5±0.2	1.0±0.1#	48.3±1.7
(b)				
H_{IGF*}	52.5±3.7#	7.4±1.0^	0.5±0.1^	80.9±0.6
H_b40_{IGF*}	16.3±1.7	15.1±2.9	0.8±0.2	70.2±4.7^
$H_b10_b40_{IGF*}$	14.3±1.6	12.9±0.4	1.3±0.1#	88.3±2.6#

For each measurement, the highest and lowest values ($p<0.05$) amongst formulations are indicated by (#) and (^), respectively.

in PBS, indicating that the use of a gelatin carrier for IGF-1 within these networks provides a means to tightly control release. It should also be noted that the final cumulative release values exhibited with composites were below the value exhibited by non-encapsulated microparticles, indicating that the OPF crosslinking procedure does not disrupt the IGF–gelatin complexation and binding.

As previously mentioned, two composite formulations were examined to assess the effect of a population of co-encapsulated, non-loaded microparticles on IGF-1 release kinetics. As shown in Fig. 2a, initially the non-loaded, 10 mM microparticles appeared to have no effect on IGF-1 release from the 40 mM microparticles as no significant differences in either the burst release values or Phase 2 release rates were observed between composite formulations in PBS (Table 4a). However, composites encapsulating microparticles crosslinked with both 10 and 40 mM GA ($H_b10_b40_{IGF*}$) eventually yielded statistically higher Phase 3 release rates and cumulative release values than constructs encapsulating only the more crosslinked microparticles (H_b40_{IGF*}). As later discussed, this trend appeared to be more pronounced in release studies conducted in CC-PBS.

3.2.2. Release in CC-PBS

In the presence of collagenase, reduced microparticle burst release was still achieved by encapsulation in a network of OPF. Likewise, composite burst release values (16.3±1.7% for H_b40_{IGF*} and 14.3±1.6% for $H_b10_b40_{IGF*}$) were dramatically lower than the burst release value from hydrogels (52.5±3.7%) in CC-PBS (Fig. 2b). However, as encapsulated microparticles were enzymatically digested by collagenase, the rate of IGF-1 release from composites began to exceed the rate of release from hydrogels. In fact, both Phase 2 and Phase 3 composite release rates were statistically higher the corresponding rates obtained with hydrogels. And by day 28, final cumulative release from $H_b10_b40_{IGF*}$ composites (88.3±2.6%) exceeded final cumulative release from hydrogels (80.9±0.6%).

More interestingly, gels encapsulating a population of less crosslinked microparticles exhibited statistically higher Phase 3 and final cumulative release values than gels only encapsulating the more crosslinked (40 mM) microparticles (see Table 4b). Specifically, the final cumulative release from H_b40_{IGF*} composites (70.2±4.7%) was intermediate to those values mentioned for hydrogels and $H_b10_b40_{IGF*}$ composites. By day 28, only fragments of $H_b10_b40_{IGF*}$ composites remained in CC-PBS, while H_b40_{IGF*} composites were in tact, yet highly swollen networks. Accordingly, the less crosslinked, non-loaded microparticles in $H_b10_b40_{IGF*}$ constructs appear to accelerate degradation and IGF-1 release, when compared to H_b40_{IGF*} and H_{IGF*} gels, by acting as digestable porogen which were quickly degraded by collagenase. A faster rate of enzymatic digestion of microparticles crosslinked with 10 mM GA (vs. microparticles crosslinked with 40 mM GA) was also observed in studies with non-encapsulated microparticles.

3.3. Dual IGF-1 and TGF-β1 release from hydrogels and composites in vitro

Two different formulations of three phase composites ($H_b10_{TGF}40_{IGF}$ or $H_{TGF}10_b40_{IGF}$) were utilized to simultaneously deliver IGF-1 and TGF-β1. The method of IGF-1 delivery was kept constant between formulations to provide a means of sustained delivery of this growth factor for approximately 4 weeks. IGF-1 release profiles from both formulations are shown in Fig. 3a (PBS) and Fig. 3b (CC-PBS). Since TGF-β1 plays a number of different regulatory roles in cartilage tissue, the method of TGF-β1 delivery was

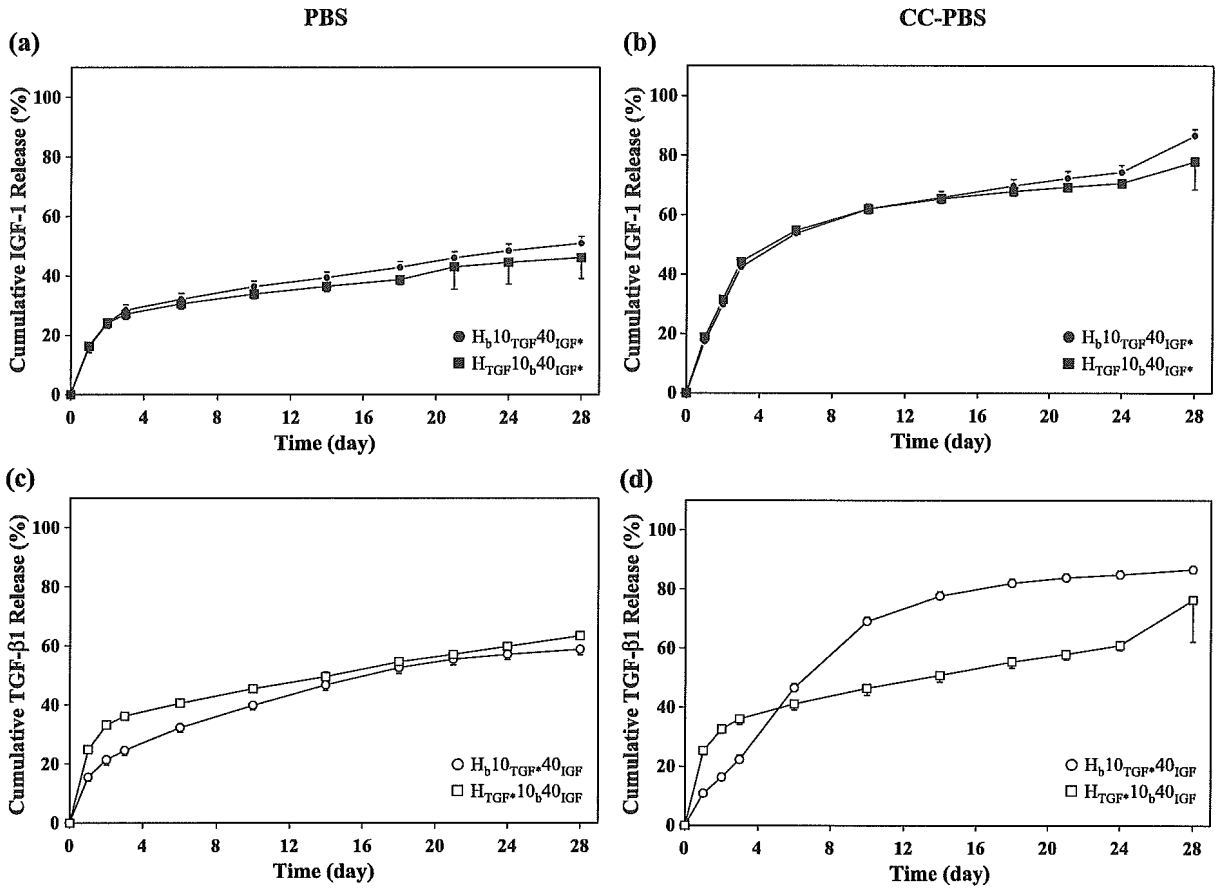

Fig. 3. OPF systems for IGF-1 and TGF-β1 delivery: (a) and (c), respectively, show simultaneous release of IGF-1 and TGF-β1 from two formulations of OPF–gelatin microparticle composites ($H_b10_{TGF}40_{IGF}$ and $H_{TGF}10_b40_{IGF}$) in PBS. (b) and (d), respectively, display IGF-1 and TGF-β1 release from these composites in CC-PBS. Error bars represent ±standard deviation of average percent cumulative release values with n=4 to 6 for each formulation. (a) and (c) PBS. (b) and (d) CC-PBS.

altered to achieve different release profiles. TGF-β1 release profiles from both formulations are shown in Fig. 3c (PBS) and Fig. 3d (CC-PBS).

3.3.1. Release in standard PBS

As shown in Fig. 3a and Table 5a, IGF-1 release proceeded in an almost identical fashion from both composite formulations in standard PBS. A burst release of approximately 16% was exhibited after 24 h, followed by Phase 2 and 3 release rates of 5–6% per day and 1% per day, respectively. Final cumulative release from both formulations was approximately 50% in PBS. In fact, no statistical differences between composite formulations were present in any of these measured parameters.

IGF-1 burst release, Phase 2 and 3 rates, as well as final cumulative release in these dual release systems ($H_b10_{TGF}40_{IGF*}$ and $H_{TGF}10_b40_{IGF*}$) were also statistically compared to respective values obtained from constructs formulated with the same material composition but loaded only with IGF-1 ($H_b10_b40_{IGF*}$). No statistical differences were seen among Phase 2 rates, Phase 3 rates, or final cumulative release values. However, the burst release (13.5±0.4%) from composites only loaded with IGF-1 ($H_b10_b40_{IGF*}$) was statistically lower than burst release from composites loaded with both TGF-β1 and IGF-1 (16.6±1.1% for $H_b10_{TGF}40_{IGF*}$ and 16.3±2.1% for $H_{TGF}10_b40_{IGF*}$), indicating that TGF-β1 loading in these composites may slightly accelerate initial IGF-1 release. A similar

Table 5
Burst release, phase 2 and 3 release rates, and final cumulative IGF-1 and TGF-β1 release from dual release systems ($H_b10_{TGF}40_{IGF}$ and $H_{TGF}10_b40_{IGF}$) in PBS (a) and in CC-PBS (b)

Gel formulation	Burst release (%)	Phase 2 rate (%/day)	Phase 3 rate (%/day)	Cumulative release (%)
(a)				
IGF-1 release				
$H_b10_{TGF}40_{IGF*}$	16.6±1.1	5.9±0.5	0.9±0.0	50.9±2.3
$H_{TGF}10_b40_{IGF*}$	16.3±2.1	5.4±0.7	0.8±0.3	46.1±7.1
TGF-β1 release				
$H_b10_{TGF*}40_{IGF}$	15.5±1.4	4.5±0.5	1.6±0.1#	58.8±1.8
$H_{TGF*}10_b40_{IGF}$	24.8±0.5#	5.7±0.6#	1.1±0.0	63.4±0.6#
(b)				
IGF-1 release				
$H_b10_{TGF}40_{IGF*}$	17.4±1.3	12.5±0.5	1.2±0.1#	86.6±2.2
$H_{TGF}10_b40_{IGF*}$	18.8±2.2	12.7±0.5	0.9±0.0	77.9±9.4
TGF-β1 release				
$H_b10_{TGF*}40_{IGF}$	10.8±0.7	5.7±0.7	2.3±0.1#	86.6±1.2
$H_{TGF*}10_b40_{IGF}$	25.2±1.5#	5.4±0.5	1.1±0.1	76.3±14.1

IGF-1 release values from composites are statistically compared ($p<0.05$) and higher values indicated by (#). The same statistical evaluation is provided for TGF-β1 release values from composites.

trend among IGF-1 burst release values was noted in CC-PBS and is discussed below.

The rate of TGF-β1 release in standard PBS (Fig. 3b) was altered by loading this growth factor within either the OPF hydrogel phase or within encapsulated 10 mM microparticles. As shown in Table 5a, when TGF-β1 was delivered from the hydrogel phase, faster overall delivery of this growth factor was achieved. In fact, burst release values, Phase 2 rates, and final cumulative TGF-β1 release values were statistically higher for $H_{TGF*}10_b40_{IGF}$ composites. Since the use of a gelatin carrier for IGF-1 was shown to greatly slow release in the absence of gelatin digesting enzymes, these results were expected for TGF-β1 and agree with previous findings [9,10].

3.3.2. Release in CC-PBS

Since these delivery systems will ultimately be used in vivo in the presence of tissue collagenase and other matrix metalloproteinases, release studies in CC-PBS may more accurately model expected release trends. Under these conditions, very similar IGF-1 release profiles (Fig. 3b) were again observed when comparing composite formulations. However, release values were higher than those observed in standard PBS. Initial burst release values from both formulations were approximately 18%, with subsequent Phase 2 release rates of approximately 13% per day (Table 5b). However, Phase 3 rates were found to be statistically different between formulations (1.2±0.1% per day for $H_b10_{TGF}40_{IGF*}$ and 0.9±0.0% per day for $H_{TGF}10_b40_{IGF*}$). Final cumulative release from $H_b10_{TGF}40_{IGF*}$ composites (86.6±2.2%) was higher, though not statistically, than cumulative release from $H_{TGF}10_b40_{IGF*}$ constructs (77.9±9.4%). Accordingly, these results may suggest that free TGF-β1 in the OPF hydrogel phase of composites may migrate and help to eventually stabilize the IGF–gelatin interactions.

Statistical comparison of IGF-1 release profiles from composites loaded only with IGF-1 ($H_b10_b40_{IGF*}$) with dually loaded composites provides further evidence that TGF-β1 may interact with IGF-1 to slightly alter release kinetics. More specifically, IGF-1 burst release values from composites loaded with both IGF-1 and TGF-β1 (17.4±1.3% for $H_b10_{TGF}40_{IGF*}$ and 18.8±2.2% for $H_{TGF}10_b40_{IGF*}$) were statistically higher than the burst release from composites loaded with only IGF-1 (14.3±1.6%). This trend was also seen in standard PBS. Thus, initially, free TGF-β1 (TGF-β1 in the OPF hydrogel phase or TGF-β1 which is not tightly complexed to gelatin) may accelerate IGF-1 release. However, in the later stages of release experiments (Phases 3 and 4), IGF-1 release from $H_{TGF}10_b40_{IGF*}$ composites was seen to be slower than release from either $H_b10_{TGF}40_{IGF*}$ or $H_b10_b40_{IGF*}$ composites. For instance, final cumulative IGF-1 release from $H_{TGF}10_b40_{IGF*}$ composites (77.9±9.4%) was statistically lower than release from $H_b10_{TGF}40_{IGF*}$ (86.6±2.2%) or $H_b10_b40_{IGF*}$ (88.3±2.6%) composites. This later trend may indicate the free TGF-β1 in the OPF hydrogel phase ultimately migrates to the gelatin phase to stabilize IGF-1–gelatin interactions. In $H_b10_{TGF}40_{IGF*}$ constructs, tightly complexed TGF-β1 may be unable to dissociate from its gelatin carrier and serve the same role.

TGF-β1 release profiles from these dual release systems are shown in Fig. 3d. Initially, significantly higher burst release was observed when TGF-β1 was loaded into the hydrogel phase of composites.

As shown in Table 5b, release after 24 h was 25.2±1.5% from $H_{TGF*}10_b40_{IGF}$ composites but only 10.8±0.7% from $H_b10_{TGF*}40_{IGF}$ composites. However by the beginning of Phase 3 (day 6), enzymatic digestion of gelatin allowed TGF-β1 release from $H_b10_{TGF*}40_{IGF}$ composites to exceed release from $H_{TGF*}10_b40_{IGF}$ composites. In fact, the Phase 3 TGF-β1 release rate for composites with TGF-β1 loading in the microparticle phase (2.3± 0.1% per day) was statistically greater than the rate for composites with TGF-β1 loading in the hydrogel phase (1.1±0.1% per day). Final cumulative TGF-β1 release from $H_b10_{TGF*}40_{IGF}$ composites rose to approximately 87%, while the corresponding value in $H_{TGF*}10_b40_{IGF}$ composites was only 76%. Accordingly, these results indicate that TGF-β1 release rates in the presence of collagenase may be systematically adjusted by altering the material phase of TGF-β1 loading.

4. Discussion

Since IGF-1 has been shown to function primarily as a progression factor, stimulating the synthesis of collagen and proteoglycans in cartilage tissue, a series of in vitro release experiments conducted to determine an effective means of providing sustained IGF-1 release over the course of several weeks. Because gelatin has been shown to form an effective ionic complexation with a number of growth factors, allowing for controlled drug delivery [29], gelatin microparticles were explored as a possible IGF-1 carrier. Initial release experiments were assessed the effect of gelatin microparticle IEP and crosslinking extent on IGF-1 release. Since gelatin is primarily degraded by enzymatic digestion, growth factors which effectively complex or bind to these microparticles will generally display release profiles with two prominent features in standard, enzyme-free PBS [10]. First, any non-complexed or poorly bound growth factor will be primarily released during the first 24 h as these microparticles reach equilibrium swelling. However, unlike diffusion controlled release systems, relatively little subsequent release may be observed due to the growth factor–gelatin complexation.

As shown in Fig. 1a and Table 3a, IGF-1 did not appear to effectively complex with basic gelatin microparticles (IEP of 9.0). However, acidic gelatin microparticles crosslinked with 10 mM GA retained approximately 68% of their loaded IGF-1 over the course of 28 days in standard PBS. Similar retention values were observed when this microparticle formulation was loaded with TGF-β1, a growth factor which has been shown to form an effective ionic complexation with acidic gelatin [29], indicating that acidic gelatin was a promising IGF-1 carrier. However, lower retention of IGF-1 in PBS was observed with acidic microparticles crosslinked with 40 mM GA. Since TGF-β1 retention in gelatin microparticles in standard PBS is not affected by their crosslinking extent [9,10], these results may suggest that the lysine and hydroxylysine amino acid residues in gelatin, which react with the aldehyde groups of GA, are also utilized in IGF–gelatin binding. Alternatively, the more tightly crosslinked network of these gelatin microparticles may prevent efficient diffusional loading of IGF-1. Yet, since decreased growth factor retention in these highly crosslinked microparticles is not observed with TGF-β1, a protein with a substantially higher molecular weight (25 kDa) than IGF-1 (7.5 kDa), it is unlikely that this behavior is due to diffusional limitations during IGF-1 loading.

However, since gelatin is enzymatically degraded, release studies in CC-PBS more accurately model expected in vivo release profiles. As shown in Fig. 1b, both basic and acidic microparticles crosslinked with 10 mM GA were rapidly digested by collagenase, releasing 90% of their IGF-1 as early as day 6. Only the more crosslinked (40 mM) acidic microparticles provided a means of sustained IGF-1 delivery over the course of 28 days in CC-PBS. Accordingly, this microparticle formulation was utilized in subsequent studies aimed at optimizing IGF-1 delivery.

More specifically, further experiments examined IGF-1 release when these microparticles were encapsulated in a network of OPF. The encapsulation procedure provides a means of maintaining microparticles within a defect site to localize growth factor delivery. Additionally, as shown in Fig. 2, encapsulated IGF-1-loaded microparticles exhibited much lower burst release values than both non-encapsulated microparticles and OPF hydrogels (with no microparticle component) in PBS and CC-PBS,

allowing for sustained IGF-1 release over the course of 4 weeks.

While release profiles from the two composite formulations were very similar, the final extent of IGF-1 release from these systems in CC-PBS was shown to be dependent on microparticle crosslinking. $H_b10_b40_{IGF*}$ composites, which encapsulated both IGF-1-loaded 40 mM microparticles and non-loaded 10 mM microparticles, exhibited statistically higher release (88.3±2.6%) than H_b40_{IGF*} composites (70.2±4.7%), which encapsulated only IGF-1-loaded 40 mM microparticles. Accordingly, the non-loaded, less crosslinked microparticles appear to speed release by acting as a porogen which is readily digested in the presence of collagenase. Furthermore, since higher final release from $H_b10_b40_{IGF*}$ composites was also observed in standard PBS, these results indicate that non-loaded microparticles do not act as a significant reservoir for IGF-1. Accordingly, by adjusting the amount and crosslinking extent of encapsulated microparticles, release kinetics may be systematically tailored.

A final set of release experiments examined dual delivery of IGF-1 and TGF-β1 from three phase composites. IGF-1 was again loaded into the 40-mM microparticle phase to allow for sustained release. However, TGF-β1 loading was varied between the 10-mM microparticle phase ($H_b10_{TGF}40_{IGF}$) and the OPF hydrogel phase ($H_{TGF}10_b40_{IGF}$). As expected, very similar IGF-1 release profiles in were observed with both composite formulations since IGF-1 was delivered from the same phase in each formulation. As discussed above, statistical comparison of IGF-1 release values from $H_b10_{TGF}40_{IGF*}$ and $H_{TGF}10_b40_{IGF*}$ composites with values from composites loaded only with IGF-1 ($H_b10_b40_{IGF*}$) indicated that the presence of co-loaded TGF-β1 slightly alters IGF-1 release. In particular, as shown in Fig. 3b, when TGF-β1 was loaded into the OPF hydrogel phase, lower final IGF-1 release was observed, indicating that free TGF-β1 may eventually diffuse to sites of IGF-1–gelatin interactions and help to stabilize this complex. While further experiments are needed to explore this phenomenon, these release systems proved successful in providing sustained release of IGF-1 with very similar release profiles. As designed, these dual release systems exhibited less than 90% final cumulative IGF-1 release in CC-PBS over a 4-week period.

As shown in Fig. 3d, altering the phase of TGF-β1 loading proved to be a successful means of altering TGF-β1 release kinetics. Significantly lower burst release (10.8±0.7%) was observed when this growth factor was released from the 10-mM microparticle phase, rather than the hydrogel phase (25.2±1.5%). Gradual release of TGF-β1 from $H_b10_{TGF*}40_{IGF}$ composites then continued as encapsulated microparticles were digested by collagenase. However, TGF-β1 release from $H_{TGF*}10_b40_{IGF}$ proceeded in a diffusion-controlled manner with a higher burst release and a steady subsequent release rate. Final cumulative release values for both systems were not statistically different at day 28. Accordingly, since the total amount of TGF-β1 released from these systems over a 4-week period was approximately equal, yet delivered via unique release profiles, implementation of these two systems in vivo would allow a means of assessing how TGF-β1 release kinetics affect tissue repair.

5. Conclusions

This research details the development of a non-invasive means of simultaneously delivering both IGF-1 and TGF-β1 to damaged articular cartilage through the use of an injectable, biodegradable scaffold comprised of the polymer OPF and gelatin microparticles. More specifically, a series of release studies assessed the effects of gelatin IEP and crosslinking extent on IGF-1 release from gelatin microparticles and demonstrated that highly crosslinked, acidic microparticles (IEP=5.0) serve as an effective carrier of IGF-1, providing sustained delivery of this progression factor over the course of 4 weeks. Furthermore, encapsulation of these IGF-1-loaded microparticles in a network of the biodegradable polymer OPF, provided a means to further control and localize release. Using these OPF–gelatin microparticle composites, dual release of TGF-β1 and IGF-1 was achieved with growth factor loading in either the microparticle phase or OPF phase of gels. Parameters such as microparticle crosslinking extent and density within these gel networks, as well as the phase of growth factor loading, provided an effective

means of controlling the release profiles of these growth factors. Accordingly, this ability provides a powerful tool by which researchers can now assess the release kinetics of one or more growth factors on tissue repair.

Acknowledgements

The work on drug delivery for articular cartilage engineering has been supported by the National Institutes of Health (R01 AR48756). T.A. Holland also acknowledges financial support by a Whitaker Foundation Graduate Fellowship.

References

[1] Center for Disease Control and Prevention, www.cdc.gov/health/ (2003).
[2] R.G. LeBaron, K.A. Athanasiou, Ex vivo synthesis of articular cartilage, Biomaterials 21 (2000) 2575–2587.
[3] E.B. Hunziker, Articular cartilage repair: are the intrinsic biological constraints undermining this process insuperable? Osteoarthr. Cartil. 7 (1999) 15–28.
[4] F.H. Silver, A.I. Glasgold, Cartilage wound healing. An overview, Otolaryngol. Clin. North Am. 28 (1995) 847–864.
[5] T.A. Holland, A.G. Mikos, Advances in drug delivery for articular cartilage, J. Control. Release 86 (2003) 1–14.
[6] S.D. Gillogly, M. Voight, T. Blackburn, Treatment of articular cartilage defects of the knee with autologous chondrocyte implantation, J. Orthop. Sports Phys. Ther. 28 (1998) 241–251.
[7] H. Shin, P.Q. Ruhe, A.G. Mikos, J.A. Jansen, In vivo bone and soft tissue response to injectable biodegradable oligo (poly(ethylene glycol) fumarate) hydrogels, Biomaterials 24 (2003) 3201–3211.
[8] J.P. Fisher, Z. Lalani, C.M. Bossano, E.M. Brey, N. Demian, C.M. Johnston, D. Dean, J.A. Jansen, M.E. Wong, A.G. Mikos, Effect of biomaterial properties on bone healing in a rabbit tooth extraction socket model, J. Biomed. Mater. Res. 68A (2004) 428–438.
[9] T.A. Holland, J.K. Tessmar, Y. Tabata, A.G. Mikos, Transforming growth factor-beta1 release from oligo(poly(ethylene glycol) fumarate) hydrogels in conditions that model the cartilage wound healing environment, J. Control. Release 94 (2004) 101–114.
[10] T.A. Holland, Y. Tabata, A.G. Mikos, In vitro release of transforming growth factor-beta1 from gelatin microparticles encapsulated in biodegradable, injectable oligo(poly(ethylene glycol) fumarate) hydrogels, J. Control. Release 91 (2003) 299–313.
[11] S.M. Seyedin, D.M. Rosen, P.R. Segarini, Modulation of chondroblast phenotype by transforming growth factor-beta, Pathol. Immunopathol. Res. 7 (1988) 38–42.
[12] M. Iwasaki, K. Nakata, H. Nakahara, T. Nakase, T. Kimura, K. Kimata, A.I. Caplan, K. Ono, Transforming growth factor-beta 1 stimulates chondrogenesis and inhibits osteogenesis in high density culture of periosteum-derived cells, Endocrinology 132 (1993) 1603–1608.
[13] M.K. Majumdar, V. Banks, D.P. Peluso, E.A. Morris, Isolation, characterization, and chondrogenic potential of human bone marrow-derived multipotential stromal cells, J. Cell. Physiol. 185 (2000) 98–106.
[14] T.I. Morales, Transforming growth factor-beta 1 stimulates synthesis of proteoglycan aggregates in calf articular cartilage organ cultures, Arch. Biochem. Biophys. 286 (1991) 99–106.
[15] G. Venn, R.M. Lauder, T.E. Hardingham, H. Muir, Effects of catabolic and anabolic cytokines on proteoglycan biosynthesis in young, old and osteoarthritic canine cartilage, Biochem. Soc. Trans. 18 (1990) 973–974.
[16] H.M. van Beuningen, P.M. van der Kraan, O.J. Arntz, W.B. van den Berg, Transforming growth factor-beta 1 stimulates articular chondrocyte proteoglycan synthesis and induces osteophyte formation in the murine knee joint, Lab. Invest. 71 (1994) 279–290.
[17] R.N. Rosier, R.J. O'Keefe, I.D. Crabb, J.E. Puzas, Transforming growth factor beta: an autocrine regulator of chondrocytes, Connect. Tissue Res. 20 (1989) 295–301.
[18] D. Vivien, P. Galera, E. Lebrun, G. Loyau, J.P. Pujol, Differential effects of transforming growth factor-beta and epidermal growth factor on the cell cycle of cultured rabbit articular chondrocytes, J. Cell. Physiol. 143 (1990) 534–545.
[19] T.I. Morales, The role and content of endogenous insulin-like growth factor-binding proteins in bovine articular cartilage, Arch. Biochem. Biophys. 343 (1997) 164–172.
[20] T. Fukumoto, J.W. Sperling, A. Sanyal, J.S. Fitzsimmons, G.G. Reinholz, C.A. Conover, S.W. O'Driscoll, Combined effects of insulin-like growth factor-1 and transforming growth factor-beta1 on periosteal mesenchymal cells during chondrogenesis in vitro, Osteoarthr. Cartil. 11 (2003) 55–64.
[21] F.P. Luyten, V.C. Hascall, S.P. Nissley, T.I. Morales, A.H. Reddi, Insulin-like growth factors maintain steady-state metabolism of proteoglycans in bovine articular cartilage explants, Arch. Biochem. Biophys. 267 (1988) 416–425.
[22] K.J. Gooch, T. Blunk, D.L. Courter, A.L. Sieminski, P.M. Bursac, G. Vunjak-Novakovic, L.E. Freed, IGF-I and mechanical environment interact to modulate engineered cartilage development, Biochem. Biophys. Res. Commun. 286 (2001) 909–915.
[23] C. Xu, B.O. Oyajobi, A. Frazer, L.D. Kozaci, R.G. Russell, A.P. Hollander, Effects of growth factors and interleukin-1 alpha on proteoglycan and type II collagen turnover in bovine nasal and articular chondrocyte pellet cultures, Endocrinology 137 (1996) 3557–3565.
[24] C.J. Wirth, M. Rudert, Techniques of cartilage growth enhancement: a review of the literature, Arthroscopy 12 (1996) 300–308.
[25] E.B. Hunziker, I.M. Driesang, C. Saager, Structural barrier principle for growth factor-based articular cartilage repair, Clin. Orthop. (2001) S182–S189.

[26] E.B. Hunziker, L.C. Rosenberg, Repair of partial-thickness defects in articular cartilage: cell recruitment from the synovial membrane, Bone Jt. Surg., Am. 78 (1996) 721–733.
[27] M.E. Joyce, A.B. Roberts, M.B. Sporn, M.E. Bolander, Transforming growth factor-beta and the initiation of chondrogenesis and osteogenesis in the rat femur, J. Cell Biol. 110 (1990) 2195–2207.
[28] Y. Tabata, S. Hijikata, M. Muniruzzaman, Y. Ikada, Neovascularization effect of biodegradable gelatin microspheres incorporating basic fibroblast growth factor, J. Biomater. Sci., Polym. Ed. 10 (1999) 79–94.
[29] M. Yamamoto, Y. Tabata, Controlled release of growth factors based on biodegradation of gelatin hydrogel, J. Biomater. Sci., Polym. Ed. 12 (2001) 77–88.
[30] E.B. Hunziker, I.M. Driesang, E.A. Morris, Chondrogenesis in cartilage repair is induced by members of the transforming growth factor-beta superfamily, Clin. Orthop. (2001) S171–S181.
[31] Y. Yoshihara, H. Nakamura, K. Obata, H. Yamada, T. Hayakawa, K. Fujikawa, Y. Okada, Matrix metalloproteinases and tissue inhibitors of metalloproteinases in synovial fluids from patients with rheumatoid arthritis or osteoarthritis, Ann. Rheum. Dis. 59 (2000) 455–461.
[32] S. Jo, H. Shin, A.K. Shung, J.P. Fisher, A.G. Mikos, Synthesis and characterization of oligo(poly(ethylene glycol) fumarate) macromer, Macromolecules 34 (2001) 2839–2844.
[33] J.S. Temenoff, H. Park, E. Jabbari, E. Conway, C. Sheffield, A.G. Ambrose, Communication: thermally cross-linked oligo(poly(ethylene glycol) fumarate) hydrogels support osteogenic differentiation of encapsulated marrow stromal cells in vitro, Biomacromolecules 5 (2004) 5–10.
[34] J.S. Temenoff, H. Park, E. Jabbari, T.L. Sheffield, R.G. LeBaron, C.G. Ambrose, A.G. Mikos, In vitro osteogenic differentiation of marrow stromal cells encapsulated in biodegradable hydrogels, J. Biomed. Mater. Res., A 70A (2004) 235–244.
[35] J. Neter, W. Wasserman, M.H. Kutner, Applied Linear Statistical Models, Richard D. Irwin, Homewood, IL, 1985.
[36] L. Lu, G.N. Stamatas, A.G. Mikos, Controlled release of transforming growth factor beta1 from biodegradable polymer microparticles, J. Biomed. Mater. Res. 50 (2000) 440–451.

Rheumatol Int (2005) 25: 553–554
DOI 10.1007/s00296-004-0559-5

CASE REPORT

Daichi Hoshina · Tadamichi Shimizu · Riichiro Abe
Junko Murata · Koichi Tanaka · Hiroshi Shimizu

Multicentric reticulohistiocytosis associated with rheumatoid arthritis

Received: 16 June 2004 / Accepted: 25 September 2004 / Published online: 12 March 2005

Abstract Due to the fact that both multicentric reticulohistiocytosis (MRH) and rheumatoid arthritis (RA) are destructive arthritic and skin disorders, it is often difficult to differentiate one from the other. Here, we report the case of a 67-year-old Japanese woman who had been diagnosed as suffering from RA 20 years ago, and who developed MRH. MRH may be misdiagnosed as RA, but evaluation of the time course of specific symptoms can greatly help in the correct diagnosis.

Keywords Multicentric reticulohistiocytosis · Rheumatoid arthritis · Distal interphalangeal (DIP) joint · Methotrexate · Malignancy

Introduction

The co-existence of multicentric reticulohistiocytosis (MRH) associated with rheumatoid arthritis (RA) is rare, and this fact may arise from difficulties in making the correct diagnoses, because both diseases involve destructive forms of arthritis and a skin disorder. In this paper, we describe a patient who was initially diagnosed with RA, but who subsequently developed MRH.

D. Hoshina · T. Shimizu (✉) · R. Abe
J. Murata · H. Shimizu
Department of Dermatology, Hokkaido University Graduate School of Medicine, Kita-ku, Sapporo, Japan
E-mail: michiki@med.hokudai.ac.jp

K. Tanaka
Section of Orthopaedics, Japan Labour Health and Welfare Organization Iwamizawa Rhosai Hospital, Iwamizawa, Japan

Department of Dermatology,
Hokkaido University Graduate School of Medicine,
Kita-ku, Sapporo, 060-8638, Japan

Case report

A 67-year-old Japanese woman had been diagnosed as suffering from RA since the age of 47 years. She had complained of pain, swelling and tenderness on her elbows, knees, shoulders and hip joints. She had previously tested positive for rheumatoid factor, and been treated with non-steroidal anti-inflammatory drugs (NSAIDs). At age 65, she developed papules on her face, especially on the ears and the dorsal aspect of the hands and fingers (Fig. 1). The papules were hard, flesh or reddish-brown colored, and ranged from 0.5 to 1.0 cm in diameter. Bilateral distal interphalangeal (DIP) joints on the hands showed subluxation and deviations on the X-ray photograph. Histopathological findings from a nodule of the finger showed diffuse, nodular invasion of histiocytes, with multiple or vesicular nuclei throughout the whole dermis (Fig. 2). Periodic acid-Schiff (PAS), lysozyme, α-1 antitrypsin and CD68 were positive in these cells, but CD1a and LCA were negative. The histopathological findings for the nodules were consistent with MRH. She was treated with methotrexate 6 mg/

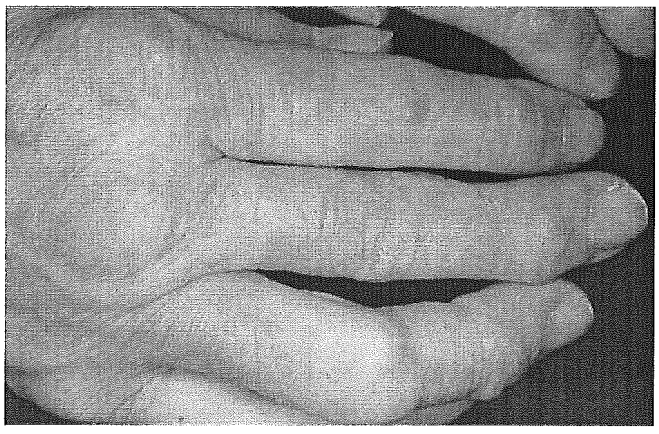

Fig. 1 Flesh to reddish-brown colored hard papules and nodules on the dorsal DIP joint of her fingers

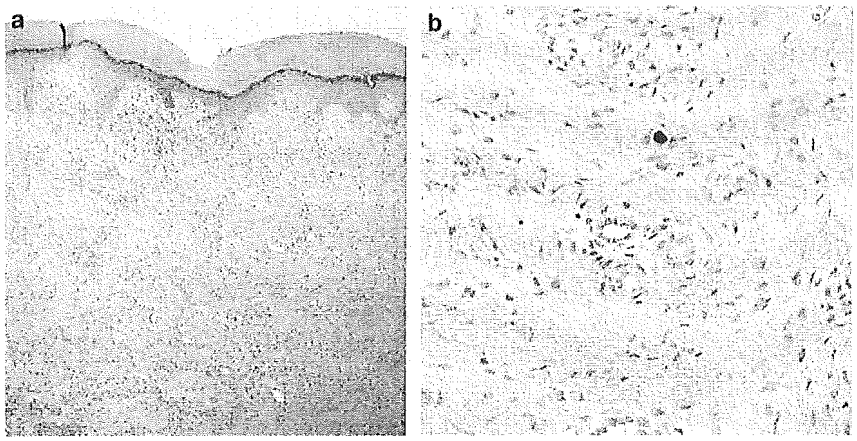

Fig. 2 Histopathology of the finger demonstrating a diffuse, nodular invasion of histiocytes, which showed multiple internal nuclei or vesicular nuclei that were distributed throughout the whole dermis. **a** low and **b** high magnification

week, in combination with prednisone 20 mg/day. The pain in the DIP joint gradually subsided, and the papules and nodules on her hands and face also gradually decreased in size over the 6 months folowing the initiation of the therapy.

Discussion

Due to the fact that both MRH and RA are destructive arthritic and skin disorders, it is often difficult to differentiate one from the other. In this case, we concluded that the patient suffered from both MRH and RA based on the following factors. The first factor was the histopathological finding of vesicles indicating MRH. The second factor was that the papules and nodules on the hand, fingers and face appeared 22 years after the symptoms of RA were first recognized, suggesting the start of a new disease pattern. The last factor in suggesting the occurrence of two distinct diseases is that DIP involvement is specific to MRH, and is considered very rare in RA [1]. Some other autoimmune diseases have been reported to be complicated with MRH. Sjögren syndrome or systemic sclerosis associated with MRH has been relatively frequently reported. This is in contrast to MRH association with RA, where only one case can be found [2]. On the contrary, some cases of MRH have been reportedly misdiagnosed as RA. Horvath and Hoffman reported a case of MRH, which was subsequently found to be misdiagnosed as RA and initially treated with naproxen and hydroxychloroquin [3].

For the treatment of MRH, the use of antiproliferative drugs could change the MRH disease course. Methotrexate, cyclophosphamide and hydroxychloroquin are well recognized as the possible treatments for MRH [4–6]. In our case, we treated the patient with methotrexate in combination with prednisone. Her DIP joint pain subsided, and the papules and nodules on her hands and face also improved. In addition, her RA-associated symptoms of pain, swelling and tenderness in her joints, also subsided after therapy.

Differentiation between MRH and RA is sometimes difficult when arthritis and skin lesion appear at the same time. However, the clinical symptoms of MRH appeared after a 20-year treatment course for RA, and we made the diagnosis of MRH associated with RA. Generally, MRH may be misdiagnosed as RA, but evaluation of the time course of specific symptoms can greatly help in the correct diagnosis.

References

1. Outland JD, Keiran SJ, Schikler KN, Callen JP (2002) Multicentric reticulohistiocytosis in a 14-year-old girl. Pediatr Dermatol 19:527–531
2. Takahashi M, Mizutani H, Nakamura Y, Shimizu M (1997) A case of muticentric reticulohistiocytosis, systemic sclerosis, and Sjogren syndrome. J Dermatol 24:530–534
3. Horvath JR, Hoffman GS (1999) Multicentric reticulohistiocytosis: a mimic of gout and rheumatoid arthritis. Cleve Clin J Med 66:166–172
4. Luz FB, Gaspar TAP, Kalil-Gaspar N, Ramos-e-Silva M (2001) Multicentric reticulohistiocytosis. J Eur Acad Dermatol Venereol 15:524–531
5. Santilli D, Lo Monaco A, Cavazzini PL, Trotta F (2002) Multicentric reticulohistiocytosis: a rare cause of erosive arthropathy of the distal interphalangeal finger joints. Ann Rheum Dis 61:485–487
6. Uhl M, Gutfleisch J, Rother E, Langer M (1996) Multicentric reticulohistiocytosis. A report of 3 cases and review of literature. Bildgebung 63:126–129

British Journal of Plastic Surgery (2005) 58, 1115-1123

ELSEVIER

BJPS
An International Journal of Surgical Reconstruction
www.bjps.com

Accelerated wound healing through the incorporation of basic fibroblast growth factor-impregnated gelatin microspheres into artificial dermis using a pressure-induced decubitus ulcer model in genetically diabetic mice

Katsuya Kawai[a,*], Shigehiko Suzuki[b], Yasuhiko Tabata[c], Yoshihiko Nishimura[d]

[a]*The Tazuke Kofukai Medical Research Institute, Kitano Hospital, 2-4-20 Ogimachi, Kita-ku, Osaka 530-8480, Japan*
[b]*Department of Plastic and Reconstructive Surgery, Graduate School of Medicine, Kyoto University, 54 Kawahara-cho Shogoin, Sakyo-ku, Kyoto 606-8507, Japan*
[c]*Institute for Frontier Medical Sciences, Kyoto University, 53 Kawahara-cho Shogoin, Sakyo-ku, Kyoto 606-8507, Japan*
[d]*Shimada Municipal Hospital, 1200-5 Noda, Shimada, Shizuoka 427-8502, Japan*

Received 14 March 2004; accepted 12 April 2005

KEYWORDS
Artificial dermis;
Basic fibroblast growth factor;
Sustained release;
Gelatin microsphere;
Decubitus ulcer;
Genetically diabetic mice;
Impaired wound healing

Abstract The objective of this study was to evaluate the effect of incorporating basic fibroblast growth factor (bFGF)-impregnated gelatin microspheres into an artificial dermis on impaired wound healing using a pressure-induced decubitus ulcer model in genetically diabetic mice.

Daily 10 h prolonged pressure at 500 g/cm^2 was loaded for 2 consecutive days over the femoral trochanter tertius of mice to produce ischemic necrosis. Five days after completion of the pressure load, the necrotic tissues were resected. Then, an artificial dermis incorporating bFGF-impregnated gelatin microspheres or bFGF in solution was implanted into the wound ($n=5$). Mice were sacrificed at 5, 7, and 10 days after implantation, and a full-thickness biopsy was taken and stained with hematoxylin and eosin for histological analysis.

All experimental animals were infected because diabetic mice have little tolerance for infection. Seven days after implantation, the incorporation of bFGF into the artificial dermis reduced infection and accelerated fibroblast proliferation and capillary formation. However, the accelerated effects were more significant

* Corresponding author. Tel.: +81 6 6312 1221; fax: +81 6 6362 0588.
E-mail address: k-kawai@kitano-hp.or.jp (K. Kawai).

S0007-1226/$ - see front matter
doi:10.1016/j.bjps.2005.04.010

with the incorporation of bFGF-impregnated gelatin microspheres than with free bFGF.

We conclude that the incorporation of bFGF-impregnated gelatin microspheres into an artificial dermis induced tissue regeneration in an artificial dermis in an impaired wound healing model.

Introduction

Recently, some growth factors and endothelial progenitor cells have been reported to accelerate wound healing.[1-5] Basic fibroblast growth factor (bFGF) can attract and stimulate the growth of fibroblasts and endothelial cells and increase the synthesis of collagenase,[6,7] and has been studied as an angiogenic factor in wound healing in humans.[8,9]

When used in vivo in the free form, bFGF cannot induce sufficient wound healing activity, because of its short half-life. Therefore, sustained bFGF release was achieved by impregnation into biodegradable gelatin microspheres.[10-12]

The effectiveness of bFGF-impregnated gelatin microspheres incorporated into artificial dermis in the healing of a full-thickness wound has been demonstrated in normal guinea pigs.[13] The incorporation of bFGF-impregnated gelatin microspheres into artificial dermis accelerated cellular proliferation, connective tissue synthesis, and finally remodelling in artificial dermis.

Genetically diabetic mice develop obesity, insulin resistance and severe hyperglycaemia. Wound healing in these mice is markedly delayed, and thought to resemble the impaired healing observed clinically in human diabetes.[14-17]

In general, the cause of decubitus ulcers is attributed to the compression of soft tissues between a bony prominence and the skin surface. Pressure applied to the body surface results in closure of the capillary circulation with necrosis of the skin and the development of ischaemic decubitus ulcers. We attempted to produce decubitus ulcers by compressing soft tissue over bony prominences in genetically diabetic mice.

In this paper, we investigated the effect of bFGF-impregnated gelatin microspheres incorporated into artificial dermis by using decubitus ulcers in genetically diabetic mice as an animal model of impaired healing.

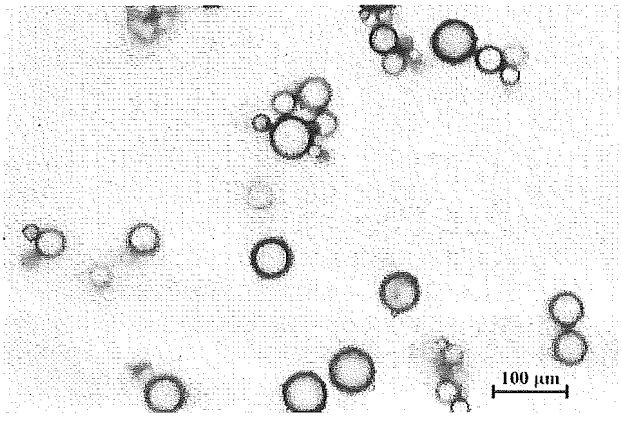

Figure 1 bFGF-impregnated gelatin microspheres with a water content of 96.75 vol%.

Materials and methods

Experimental materials

An aqueous solution of human recombinant bFGF with an isoelectric point of 9.6 (10 mg/ml) was supplied by Kaken Pharmaceutical Co., Ltd, Tokyo, Japan. The gelatin sample used, isolated from bovine bone by an alkaline process, had an isoelectric point of 4.9 and a molecular weight of 99 000 (Nitta Gelatin Co., Osaka, Japan). Artificial dermis (Pelnac®; Gunze Co., Kyoto, Japan) composed of an outer silicone layer and an inner collagen sponge layer with a pore size of 70-110 μm and pore volume fraction of 80-95% was used.

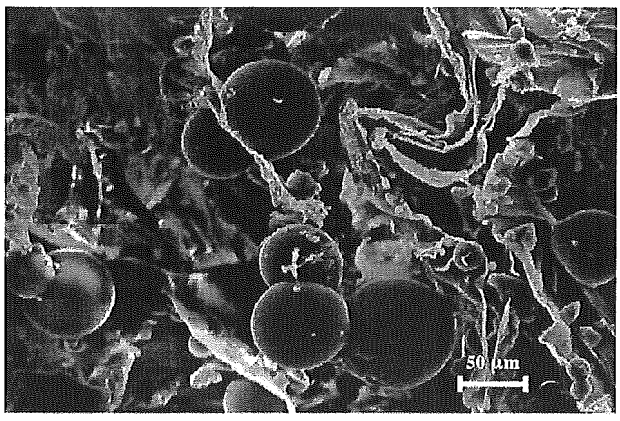

Figure 2 Scanning electron microscopic view of an artificial dermis containing gelatin microspheres. The average pore size of the artificial dermis was 70-110 μm and the gelatin microsphere average diameter was 60 μm.

Preparation of bFGF-impregnated gelatin microspheres

Gelatin microspheres were prepared through glutaraldehyde crosslinking of a gelatin aqueous solution as reported previously.[12] The water content of the gelatin microspheres used in this study was 96.75 vol%. The microsphere average diameter after swelling in saline was approximately 60 μm ranging from 32 to 86 μm (Fig. 1).

Basic FGF-impregnated gelatin microspheres were obtained by dropping 20 μl aqueous solution containing bFGF onto 2 mg freeze-dried gelatin microspheres, following by standing at room temperature for 30 min to allow bFGF to impregnate into the dried microspheres.

Incorporation of gelatin microspheres into artificial dermis

Gelatin microspheres (2 mg) impregnated with bFGF were suspended in 0.2 ml saline. The gelatin microsphere suspension was uniformly injected into several portions of the inner collagen sponge of the artificial dermis. As a control, 0.2 ml saline with or without bFGF was also injected into the collagen sponge layers. The bFGF doses were 50 μg/sponge. The doses used in this study were based on our own preliminary dose-response studies.[13]

The scanning electron microscopic structure of the artificial dermis incorporating gelatin microspheres is shown in Fig. 2.

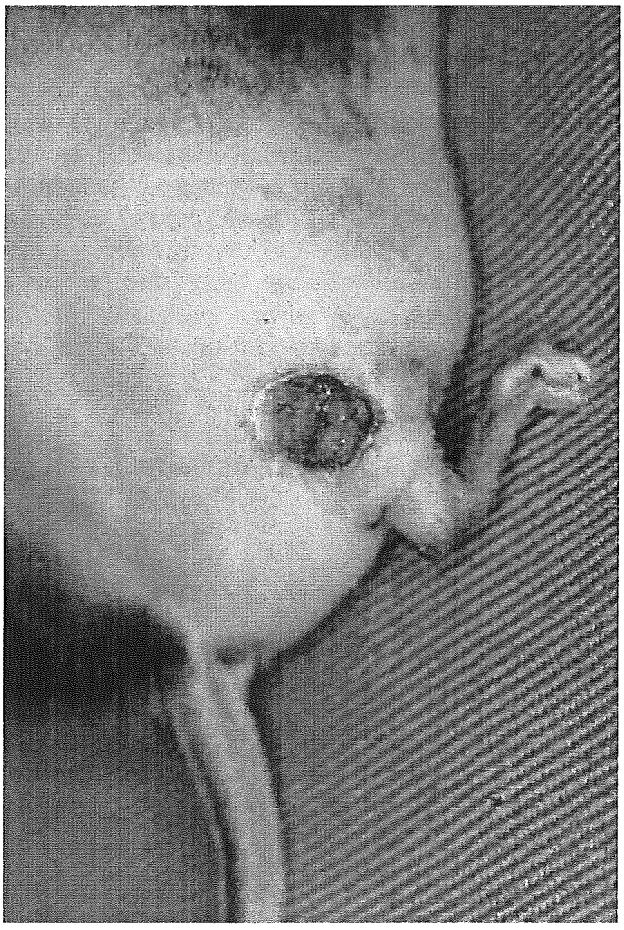

Figure 3 The ischaemic lesion 5 days after completion of the pressure load.

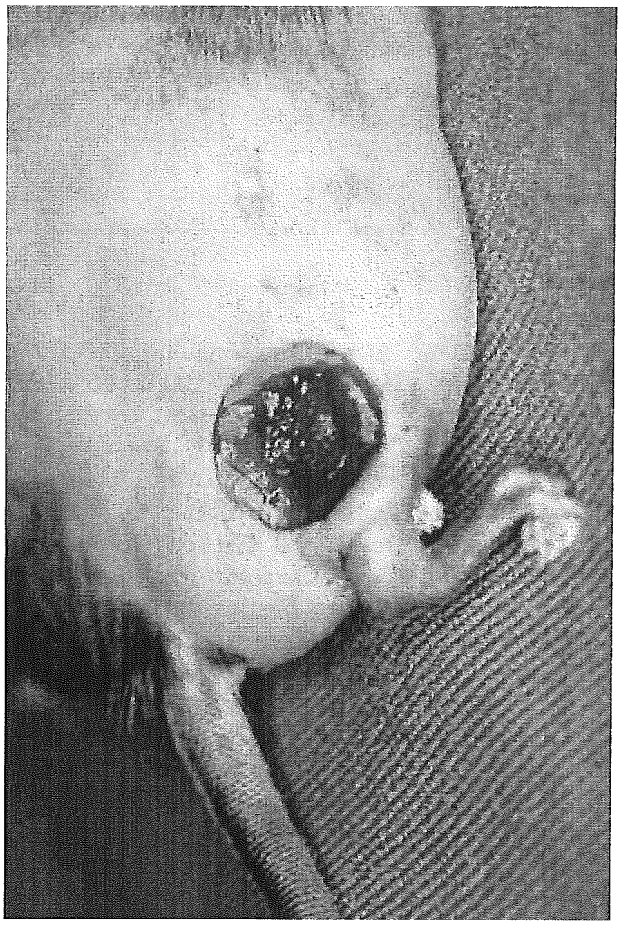

Figure 4 The necrotic tissue was resected.

Pressure-induced decubitus ulcer model in diabetic mice

Animals; genetically diabetic (C57BLKS/J-db/db) female mice aged 9 weeks were purchased from CLEA Japan, Inc., Japan. All mice were checked for urinary glucose by reagent strips. All mice were judged to be mildly to severely diabetic.

These mice were shaved and depilated under anaesthesia with ether, and then positioned on the experimental table. To produce ischaemic necrosis, daily 10 h prolonged pressure at 500 g/cm^2 was loaded for two consecutive days over the femoral trochanter tertius of mice with a pneumatically

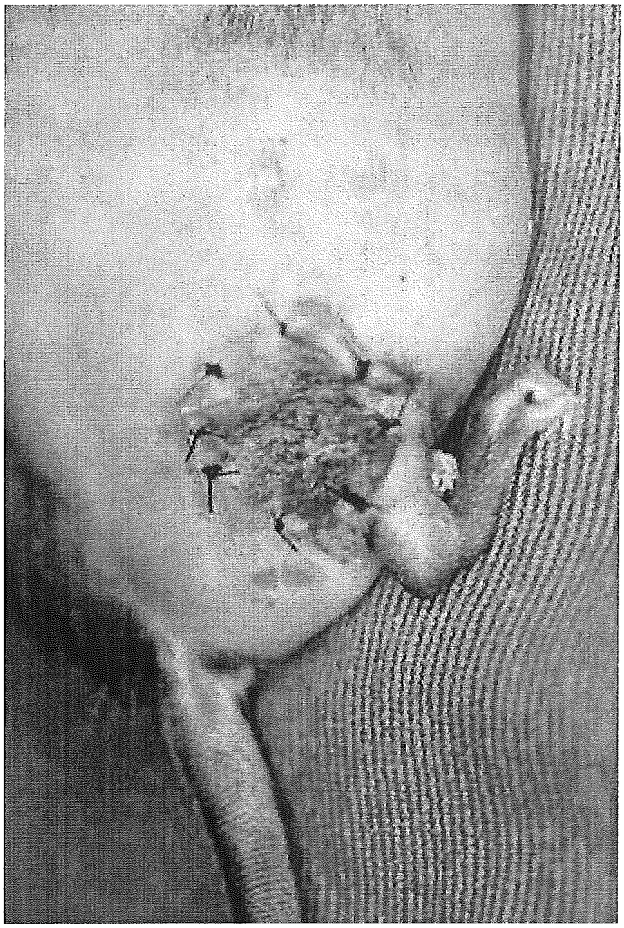

Figure 5 The artificial dermis was implanted into the wound.

driven compressor. Air pressure was regulated with a precision regulator providing a constant pressure level. Five days after removal of the pressure load, the necrotic tissues were resected (Fig. 3). The resulting wound reached to the femur with full-thickness ulcers extending from the skin through to the bone (Fig. 4).

Implantation of artificial dermis containing bFGF-impregnated gelatin microspheres

Forty-five mice were divided into three groups: (1) sustained release group; artificial dermis containing bFGF-impregnated gelatin microspheres, (2) single application group; artificial dermis containing bFGF and (3) control group; artificial dermis without bFGF. The dose of bFGF was 50 μg/sponge. After debridement of the necrotic tissues, the sponges were implanted into the resulted wounds and sutured to the wound edge with a 5/0 nylon monofilament (Fig. 5). All the wounds were covered with gauze containing fradiomycin sulfate, and the edges of the gauze were sutured to the skin with a 4/0 nylon monofilament.

Assessment of fibroblast proliferation and new capillary formation in the artificial dermis

Mice were sacrificed 5, 7, and 10 days after implantation (5 mice/group/day), and the implanted artificial dermis and the surrounding tissue were harvested. For histological examination, the tissue specimens were fixed in 10% neutral-buffered formalin solution, embedded in paraffin wax, sectioned at two selected areas of each sample (central, and adjacent sites) (3 μm thickness), and stained with haematoxylin and eosin. These sections were viewed microscopically to evaluate the proliferation of fibroblasts and the formation of new capillaries in the collagen sponge layer of the artificial dermis.

Photomicrographs of the histological sections were taken at a magnification of 100 from the bottom to top layer of the artificial dermis in the central areas of each specimen to count the number of infiltrated fibroblasts and newly formed capillaries. All observation and counting were performed by one investigator, and the final number of fibroblasts and capillaries was based on the average after counting twice.

Statistic analysis

All data were analysed by Student's *t*-test and expressed as the mean $\pm$ standard error. A value of $p < 0.01$ was accepted as statistically significant.

Results

Macroscopic tissue appearance

Fig. 6 shows the tissue appearance 7 days after implantation of the artificial dermis. In the control group, the collagen sponge was completely degraded because of infection. In the single application group, degradation of the collagen sponge was suppressed and regenerated connective tissue was slightly observed, although infection still remained. However, in the sustained release group, infection had subsided and tissue regeneration was accelerated.

Histological evaluation

Five days after implantation, the infiltration of